Behaviour and Modeling of Cup Anemometers under Icing Conditions

Dr. Guy Fortin and Prof. Jean Perron and Prof. Adrian Ilinca
Post Doctoral, Engineering Department, Université du Québec à Rimouski
300, allée des Ursulines, G5L 3A1, gfortin@uqac.ca

***Abstract*— Cup anemometers are used in the wind energy industry to characterize wind farm sites and to predict monthly and annual energy production. Their role is important, since wind speed predictions depend on their correct operation. Unfortunately, northern climates greatly affect the performance of anemometers, because in-cloud icing generally occurs at higher altitudes (more than 600 m). Wind speed prediction error caused by rime ice accreted on the anemometer can be as large as 10 % to 30 % during the winter months. This generates big errors in wind predictions, resulting in an undervaluation of the wind potential of a site or causing overloads to the wind turbines which depend only on the parameters read by the anemometer. In order to partially remedy this difficulty, heated cup anemometers are used. The Anti-icing Materials International Laboratory (AMIL) at the University of Quebec at Chicoutimi (UQAC), in collaboration with the Wind Energy Group at the University of Quebec at Rimouski (UQAR) evaluated, in a refrigerated wind tunnel, under a very severe freezing fog, the behaviour of two cup anemometers in order to estimate and model performance loss in adverse atmospheric conditions. The results obtained show that performance decreases for both unheated and heated cup anemometers with respect to exposure time and freezing fog severity, leading to complete stoppage of the unheated anemometer. Finally, a semi-empirical equation, taking into account air speed and temperature, liquid water content as well as water droplet median volumetric diameter is proposed in order to predict a cup anemometer's performance loss due to exposure time to freezing fog.**

I. Nomenclature

Ac	:	Accumulation parameter	
d_c	:	Cylinder diameter	m
d	:	Cup diameter	m
e_{ice}	:	Ice thickness	m
E	:	Collection efficiency	
f	:	Solid fraction	
L	:	Cylinder length	m
LWC	:	Liquid water content	g/m^3
m_{ice}	:	Ice mass	kg
MVD	:	Median volumetric droplet diameter	μm
t	:	Exposure time	s
T	:	Wind tunnel air temperature	K
T_f	:	Water freezing temperature	K
U	:	Wind tunnel air speed	m/s
U_m	:	Measured air speed	m/s
ρ_{ice}	:	Ice density	kg/m^3
τ	:	Dimensionless time parameter	$s\,(kg/m^3)^{-0.577}\,\mu m^{-0.814}\,K^{-0.39}$

II. Introduction

Often, the best sites for wind farm installation are situated at altitude because of an increase in wind speed of approximately 0.1 m/s per 100 m of altitude for the first 1000 m. This increase is significant since wind energy varies with the cube of the wind speed. In northern climates, the available wind power can rise by more then 10 % due to increased air density at lower temperatures. In Northern Europe (Finland, Sweden and Norway), in mountainous regions in Central Europe and in Northern America (Vermont and Alaska in USA, Yukon in Canada), the literature [1] shows that operating wind turbines at high altitude, between 1000 m to 3000 m, is particularly difficult due to icing, especially at more northern latitudes. Some problems typically encountered are directly related to the functioning of measuring instruments, particularly anemometers.

Cup anemometer sensors are sensitive to ice accumulation. The measured wind speed can be reduced by about 10-30 % due to ice accumulation. Inadequate wind direction measurements can also be a result [2]-[3]. This is as serious a problem for wind energy assessment as for the operation of wind farms. The anemometer and wind vane icing reduce wind energy production and can cause problems in the operation of wind farms. Aarnio and Partonen [4] report minor faults in hydraulic systems, anemometers and the blade heating systems control at the Lammasoaivi arctic wind farm in Finland. This sometimes resulted in production stoppage when the air temperature was lower than the turbine limit operating temperature (-25 °C). In very hostile climates, such as Acqua Spruzza, 1350 m above sea level (asl) in the Apennines in Italy, with 12 to 36 equivalent icing days per year, Botta, Cavaliere and Holttinen [5] report that occasionally wind turbines are put in stand-by mode due to heavy ice accretion on the blades. The wind turbine monitoring operation and climatic conditions (wind intensity, air temperature, icing, solar radiations, and humidity sensors) show that the anemometer and the wind vane mounted on the nacelle iced before the blades, leading to improper turbine operation. Maissan [6] has reported the same problem in the extremely hostile climate of Whitehorse, located in south central Yukon in Canada at 1430 m asl, with 33 to 50 equivalent icing days per year. Despite using heated anemometers, the wind vanes were still immobilized by ice and were replaced by fully heated Hydro-Tech instruments.

The ice detector supplied with the turbine was not effective and was removed from the control circuit. Schönborg and Blomgren [7] have reported similar problems in Rodovalen (883 m asl) in the Swedish Alps, where high humidity caused heavy rime on heated anemometers and wind vanes. Schaffner [8] summarizes his experience gained during a measurement campaign for wind energy site assessments in the Swiss Alps over the last 15 years. The unheated cup anemometers failed 30-95 % of the time during winter at alpine sites, depending on anemometer type, altitude and weather conditions. He suggested the use of heated sensors, as well as anemometer cups and shafts in order to prevent ice accumulation.

In Quebec, a good example of this kind of site is the 108 MW wind farm that 3CI operates on Mount Copper and Mount Miller at an altitude of about 1000 m near Murdochville. Presently, five 1.8 MW VESTAS wind turbines are in operation. The city is bordered on three sides by the Saint-Lawrence estuary causing long periods of in-cloud icing during wintertime and results in high rime ice accumulation [9]. Taking into account the high altitude icing problems described in the European literature and the difficulties encountered at the 3CI wind farm in Murdochville, the Wind Energy Group at UQAR, in collaboration with the AMIL at UQAC have installed, in November 2004, a weather station to study the impact of rime ice on meteorological instruments. It is situated at the old Noranda mine site in Murdochville. The Gaspé Wind Energy TechnoCentre financed the station and started a project to implement an Integrated Research Centre and Technology Transfer on Wind Energy in Nordic Climates. Before the installation of the weather station, it was decided to evaluate the performance of anemometers under severe icing precipitation, simulated in a refrigerated wind tunnel. Two cup anemometers made by NRG Systems were tested, the unheated #40 and the first generation Ice-free Electrically Heated Anemometer.

The purpose of this paper is to quantify the NRG cup anemometer performance degradation and to provide a dimensionless equation to estimate the true air speed as a function of the wind speed measured by the anemometer, the liquid water content in the air and the precipitation time duration during in-cloud icing.

III. Methodology

A. Cup Anemometers

The NRG#40 anemometer consists of 3 conical cups, 2 inches in diameter. The overall assembly dimensions are 3.2 inches in height and 7.5 inches in diameter. The cups consist of one-piece injection-moulded black polycarbonate and ABS plastic housing (**Figure 1 a**). The operating speed range is from 1 m/s to 96 m/s and temperature range is from –55 °C to 60 °C. The first generation Ice-free Electrically Heated Anemometer, now 8 years old, also consists of 3 cups (**Figure 1 b**). The overall assembly dimensions are 11 inches in height and 5 inches in diameter. The anemometer head is one-piece cast aluminium with a black anodized finish and heat resistant black paint. The operating speed range is from 1.1 m/s to 90 m/s and temperature range is from –40 °C to 80 °C. The heater is 24V DC with amperage between 1.5 and 6 Amperes. This maintains the anemometer head at a temperature of 140 °C at an ambient temperature of 21 °C.

a b

Fig. 1. Cup anemometers: a) NRG#40 and b) NRG first generation Ice-free Electrically Heated Anemometer.

B. Procedure

The experimental test was conducted at the AMIL refrigerated wind tunnel under three icing precipitation conditions controlled in speed (± 0.5 m/s), temperature (± 0.5 °C) and liquid water content (± 0.03 g/m³) as presented in **Table I**. A dry ice accretion regime occurs under all three conditions.

TABLE I
EXPERIMENTAL CONDITIONS

Condition	Wind tunnel speed (m/s)	LWC (g/m^3)	Temperature (°C)
1	5	0.55	-10
2	10	0.40	-10
3	15	0.28	-10

C. AMIL Wind Tunnel Description

The AMIL refrigerated wind tunnel is a low speed wind tunnel able to operate at subzero temperatures. The tunnel is in a closed loop configuration (**Figure 2**) of 11 m long by 5.5 m wide and 3 m high. The convergent is 2.86 m long and the upstream and downstream sections are 4.5 m^2 and 0.28 m^2 respectively. The test section is 1 m long x 0.5 m wide and 0.6 m high. A BUFFALO Type S fan connected to a 100 HP motor (1800 rpm) produces a wind velocity in the test section of up to about 85 m/s, a velocity ramp of up to 10 m/s^2, uniformity better than 1.5 % and turbulence intensity less than 0.5 %. The air temperature can be controlled down to about -30 °C by passing through a double row of fine tubes cooled by a three-stage refrigeration system (freon-water, freon-glycol and air-glycol) powered by a 75 HP compressor and a glycol pump. When it is necessary, liquid nitrogen is added to the airflow to cool it down to -50 °C.

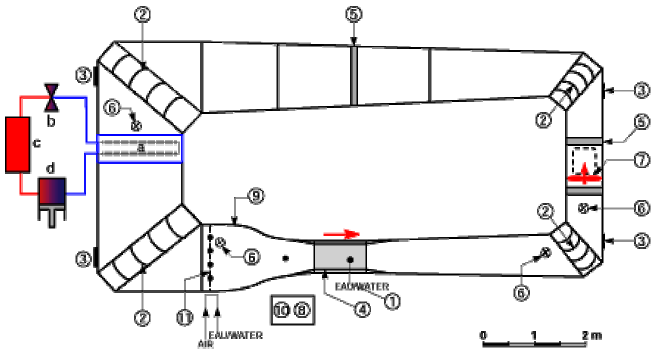

1	SECTION D'ESSAI TEST SECTION		SYSTÈME DE RÉFRIGÉRATION REFRIGERING SYSTEM
2	DÉFLECTEURS DE COIN CORNER VANES	a	ÉVAPORATEUR EVAPORATOR
3	PORTES D'ACCÈS ACCESS DOORS	b	SOUPAPE DE DÉTENTE EXPANSION VALVE
4	PANNEAUX D'ACCÈS ACCESS PANELS	c	CONDENSEUR CONDENSOR
5	JOINTS FLEXIBLES THERMAL EXPANSION JOINTS	d	COMPRESSEUR (75 hp) COMPRESSOR (75 hp)
6	DRAINS DRAINS		
7	MOTEUR ET VENTILATEUR FAN AND MOTOR		
8	PANNEAU DE CONTRÔLE MOTOR CONTROL PANEL		
9	CONVERGENT CONTRACTION CONE		
10	CONSOLE DE CONTRÔLE CONTROL CONSOLE		
11	GICLEURS SPRAY NOZZLES		

Fig. 2. AMIL wind tunnel.

D. Liquid Water Content Calibration

An aluminium rotating cylinder, one inch in diameter ***d***, and 19.4 inches long ***L*,** was used to measure the liquid water content ***LWC*** in the center of the wind tunnel test section. All tests were run at an air temperature of -10 °C at one rotation per minute for the dry ice accretion regime.

The collection efficiency ***E***, of the rotating cylinder was calculated for the full range of airspeeds and droplet sizes used in this test with the Walton and Woolcock [10] collection coefficient. The effect of droplet size was also investigated, but no significant effects were found within the droplet size range of 14 to 50 µm. The median volumetric droplet diameter ***MVD*** measured and used to calculate the collection efficiency was 27 µm. After the tunnel temperature and desired airspeed were stabilized, the water spray was turned on at the desired air and water pressure for 60 min. The ice thickness e_{ice}, on the cylinder was measured using a chilled micrometer and the ice mass m_{ice}, was measured with a chilled balance. The measured ice mass m_{ice} and thickness e_{ice}, exposure time ***t***, and wind tunnel air speed ***U*,** were used in the equation below to estimate the liquid water content ***LWC*** [11].

$$LWC = \frac{m_{ice}}{E \cdot U \cdot t \cdot L \cdot \left(d_c + e_{ice}\right)} \qquad (1)$$

E. Icing Precipitation Simulation

The icing precipitation simulation was according to the following sequence. The anemometer was installed at the center of the wind tunnel test section. After the tunnel temperature and desired airspeed were stabilized, the water spray was turned on at the desired air and water pressure for 30 min. Once the precipitation was stopped, the ice thickness was measured with a chilled micrometer and a picture was taken. The same procedure was repeated, but the experiment was stopped either after 180 min or when the cup anemometer stopped. During each run, the wind tunnel air speed and temperature, as well as the cup anemometer speed was monitored at one second intervals.

IV. Dimensionless Procedure

The experimental results obtained can only be used for the specific conditions under which they were obtained, unless a scaling procedure yields dimensionless results so that the true air speed can be estimated with a semi-empirical equation. In this section, a semi-empirical dimensionless equation is developed to estimate the air speed based on the measured iced cup anemometer speed when the air temperature, the liquid water content and the median volumetric droplet diameter are known. This semi-empirical relation is developed using a simple dimensionless model adapted to the cup anemometer.

The most important parameter for the cup anemometer dimensionless procedure is the liquid water collected. The scaling of liquid water content should be respected when the ice thickness is the same in both scaled and referenced cases. After the normalisation of the ice thickness by the cup diameter, the accumulation parameter ***Ac***, [12]-[13] can be expressed in terms of the liquid water content ***LWC***, wind tunnel air speed ***U***, exposure time ***t***, solid fraction ***f***, cup diameter ***d*** and ice density ρ_{ice}.

$$Ac = \frac{LWC \cdot U \cdot t}{f \cdot d \cdot \rho_{ice}} \qquad (2)$$

The exposure time scaling ***t*** should be respected when the accumulation parameter is the same in both the scaled and referenced cases. For a dry regime accretion, the solid fraction is 1 and the scaling equation is:

$$\frac{LWC_S \cdot U_S \cdot t_S}{d_S \cdot \rho_{ice-S}} = \frac{LWC_R \cdot U_R \cdot t_R}{d_R \cdot \rho_{ice-R}} \qquad (3)$$

When the ice mass is the same in the scaled and referenced cases, the profile in the dry regime for both cases should be similar if the ice densities are the same. According to Jones [14], the most important parameter in ice density is the Jones parameter expressed in term of cup diameter ***d***, wind tunnel air speed ***U***, liquid water content ***LWC***, median volumetric droplet diameter ***MDV*** and wind tunnel air temperature ***T***.

$$S = \frac{d^{0.82} \cdot U^{0.59} \cdot LWC^{0.21}}{MVD^{0.48} \cdot (T_f - T)^{0.23}} \qquad (4)$$

The scaling of speed ***U*,** should be respected in the dry regime when the Jones parameter ***S***, [14] is the same in the scaled and referenced cases. For a dry regime accretion, the scaling equation is:

$$\frac{d_S^{0.82} \cdot U_S^{0.59} \cdot LWC_S^{0.21}}{MVD_S^{0.48} \cdot (T_f - T_S)^{0.23}} = \frac{d_R^{0.82} \cdot U_R^{0.59} \cdot LWC_R^{0.21}}{MVD_R^{0.48} \cdot (T_f - T_R)^{0.23}} \qquad (5)$$

The last term to be considered in the cup anemometer scaling procedure is the thermal term [13]. It should have a similar thermal situation and accretion regime in the scaled and referenced cases. The thermal situation is the same in both cases when the surface temperatures in the dry regime are the same. To simplify the model, the thermal term is neglected and the scaled and referenced cases are assumed to have the same thermal situation. The wind tunnel air speed in the exposure time scaling equation is eliminated in the dry regime by combining the time and speed scaling equations. Knowing that the scaled and referenced cases have the same cup diameter and ice density, the time scaling equation that describes the accumulation parameter and the ice profile is:

$$\frac{t_R}{t_S} = \left(\frac{LWC_S}{LWC_R}\right)^{0.577} \left(\frac{MVD_S}{MVD_R}\right)^{0.814} \left(\frac{T_f - T_S}{T_f - T_R}\right)^{0.39} \qquad (6)$$

For the conditions studied, the median volumetric droplet diameter and the wind tunnel air temperature are constant, and the dimensionless equation is simplified to

$$\frac{t_R}{t_S} = \left(\frac{LWC_S}{LWC_R}\right)^{0.577} \qquad (7)$$

V. Results

The wind tunnel air speed measured by the cup anemometer as a function of time is presented in **Figure 3** for the NRG#40 and the ice-free NRG cup anemometer. The average wind tunnel speed is presented in **Table 2**.

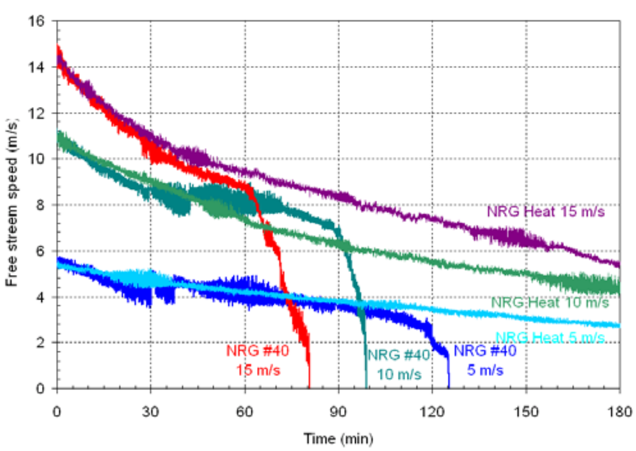

Fig. 3. Measured wind tunnel air speed as a function of time.

TABLE II
WIND TUNNEL AVERAGE AIR SPEED

Experiment	Average wind tunnel speed (m/s)	
	NRG#40	Ice free heated NRG
1	5.39	5.54
2	10.14	10.39
3	15.07	14.71

For both cup anemometers, the speed decreases with the time due to ice accumulation on the head and the cups (**Figure 4 a and b**). The ice which covers the cups is milky, a characteristic of rime ice observed in a dry accretion regime. The ice accumulation increases the cup drag and decreases the anemometer rotation or the frequency, which decreases the measured wind tunnel air speed compared to the actual wind tunnel air speed. For the NRG#40, the ice accreted on the anemometer body (**Figure 5 a**) stopped the cup rotation after a period of time. The time before stoppage depends on liquid water content and wind tunnel speed. For the ice-free NRG cup anemometer, the heating system melted the ice on the anemometer body, thus preventing ice from forming there (**Figure 5 b**). The heating system allowed head rotation to be maintained. However, because of ice accumulating on the cups, the measured wind tunnel air speed was lower then the actual wind tunnel air speed, same as for NRG#40.

a b

Fig. 4. Iced cups at 10 m/s after 60 min a) NRG#40 and b) NRG first generation Ice-free Electrically Heated Anemometer.

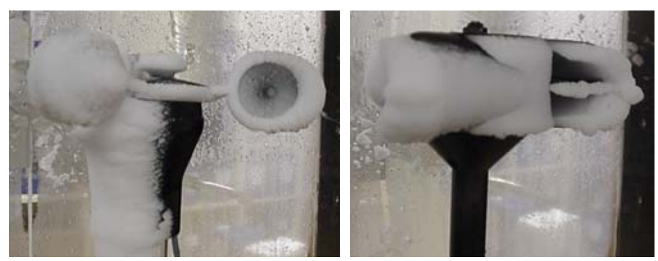

a b

Fig. 5. Iced cups at 10 m/s a) NRG#40 at 100 min. and b) NRG first generation Ice-free Electrically Heated Anemometer at 180 min.

The performance degradation in time for both anemometers is similar during the initial period of accretion. However, for the NRG#40, the degradation accelerates very fast, resulting in a complete stoppage of the anemometer in a short time period. An increase in the tunnel wind speed and the liquid water content leads to an even shorter functioning period for the NRG#40 cup anemometer. This is because at higher speeds the liquid water collected by the anemometer increases, as it is proportional to the liquid water content of the air multiplied by the wind tunnel speed.

The ice thickness evolution in time is shown in **Figure 6**. The ice thickness increases almost linearly with time. However ice thickness seems to grow more linearly on the ice-free NRG cup anemometer than on the NRG#40. The NRG#40 cup anemometer stopped rotating once 10 mm of ice formed. But the stoppage took place at different times because at lower speeds more time is needed to collect the same amount of ice. By comparing the ice thicknesses for both cup anemometers, at the same air speed and time, the ice-free NRG showed a thicker accumulation than the NRG#40. Thus the collection efficiency coefficient associated with the ice-free NRG shape is greater than for the NRG#40. This is due to the larger diameter of the ice-free NRG.

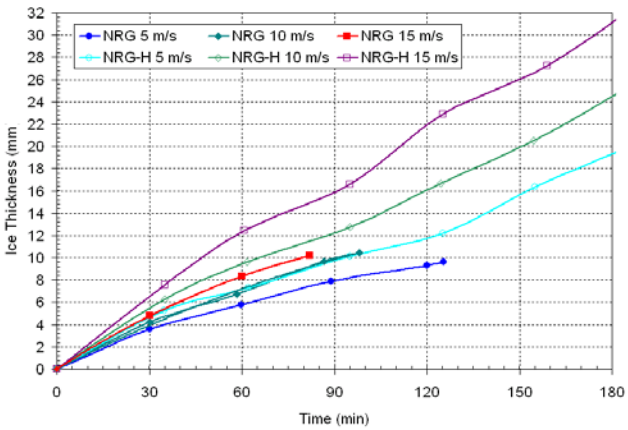

Fig. 6. Ice cup thickness as a function of time.

Using the proposed dimensionless equation, it is possible to present all experimental results in the same form. For each case, the referenced parameters are replaced by the experimental value and the dimensionless speed is plotted as a function of the scaling parameter as shown in **Figure 7**. Each case behaves in approximately the same way using dimensionless values. Rotation of the NRG#40 stops at the same abscissa value. The head rotation for the NRG#40 decreases very fast after 4.5 for 15 m/s and 5.2 for the other speeds and at 6, the head rotation stops.

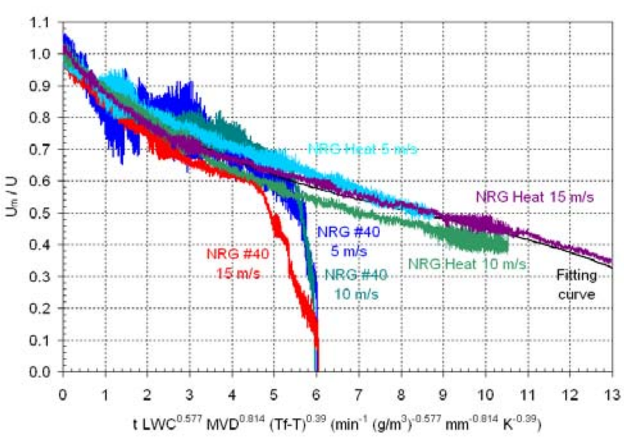

Fig. 7. Dimensionless measured wind tunnel air speed as a function of dimensionless time parameter.

The behaviour of both anemometers is similar in dimensionless form because the ice accumulated on both types of cups is equivalent (**Figure 8**). The ice thickness as shown in **Figure 8** grows at the same rate for both the NRG#40 and ice-free NRG anemometers due to a similar collected liquid water mass. The NRG#40 anemometer stops at the same dimensionless time for all cases when the same ice mass is accumulated. In time unit, the accumulation time decreases when the wind speed increases. For the ice-free NRG anemometer, the ice thickness increases with time due to the fact that collected liquid water mass increases when the wind speed increases for the same accumulation time.

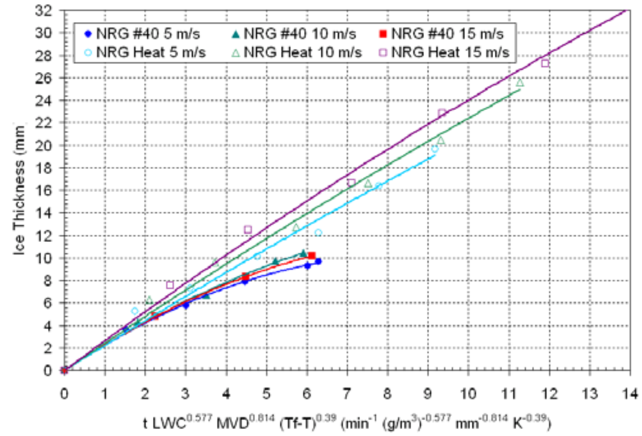

Fig. 8. Dimensionless measured ice thickness as a function of dimensionless time parameter.

The speed degradation can be easily quantified with the curve presented in **Figure 7,** because each case behaves similarly. Speed degradation increases with an increase in time. The maximum error measured for wind speed is 60 % for the ice-free NRG while for the NRG#40, the maximum error reached 40 % just before it stopped rotating.

VI. DISCUSSION

The method developed and used to render the data dimensionless provides similar results for all 6 cases evaluated in this paper. The average error is 10 % for the ice-free NRG cup anemometer on the whole data range and 11 % for the NRG#40 cup anemometer for the data ranging between 0 and 4.5. An acceptable error, since the error of icing profile reproduction in a wind tunnel is of the same order of magnitude.

The ice-free NRG and the NRG#40 cup anemometer have the same speed degradation and the speed error measurement, which increases with the accumulation time or the ice accreted. An equation to estimate the true speed from the measured value by the cup anemometer can be obtained by fitting the data with a least squares method. The best data fit is obtained with a polynomial of order 3 (R=0.95) and the fitting curve is shown in Figure 7. Equation (8) for true speed is expressed in terms of the measured speed $\boldsymbol{U_m}$ and time parameter τ.

$$U = \frac{U_m}{-3.9826\times10^{-4}\tau^3 + 1.0239\times10^{-2}\tau^2 - 1.1758\times10^{-1}\tau + 1} \quad (8)$$

where

$$\tau = t \cdot LWC^{0.577} \cdot MVD^{0.814} \cdot \left(T_f - T\right)^{0.39} \quad (9)$$

For the NRG#40, the equation (8) is valid for $\tau < 5$.

The Ice-free Electrically Heated Anemometer is sold as remaining ice free, to be used in severe wind and icing condition. However, for the experimental conditions tested in this paper, the heating is insufficient. Because the liquid water content limit of the heated anemometer is unknown, the reliability cannot be discussed based on presented data. To determine the heating system reliability of the first generation Ice-free Electrically Heated Anemometer, now 8 years old, its heating parameter was checked. The inside head temperature was 100 °C at 1 A and 24 V at an ambient temperature of 20 °C. The outside surface head temperature without rotation was 62 °C. These results are below the stated anemometer parameters, which are a head temperature of 140 °C at 1.4 A and 24 V at an ambient temperature of 20 °C. To make sure that the problem is not linked to the age of the mechanism, a second generation Ice-free Electrically Heated Anemometer was bought and tested. The second heating test also gave results below expected, namely an inside head temperature of 110 °C at 1 A and 24 V at an ambient temperature of 20 °C. The outside surface head temperature without rotation was 65 °C.

VII. CONCLUSIONS

Experimental work is presented in this paper to analyse the behaviour of two anemometers during severe icing conditions. The first generation Ice-free Electrically Heated Anemometer cannot be used to measure true wind speed in the field under severe icing conditions. Its performance degradation increases with icing time. The maximum error on the measured speed for the ice-free NRG anemometer was 60 %. The maximum error for the NRG#40 cup anemometer reached 40 % before it stopped working.

The dimensionless analysis of the results provided a good empirical correlation between the real wind speeds and those measured by the anemometers during ice accretion. All six experimental tests made at different wind speeds and liquid water content conditions fitted well with a polynomial regression. When the liquid water content, the median volumetric droplet diameter and the air temperature are known, the wind speed measured by the NRG cup anemometer can be corrected to estimate the true wind speed with the semi-empirical correlation within a 10 % error.

VIII. RECOMANDATIONS

To measure wind speed at the Murdochville weather station, the NRG sensor should be used in combination with a heated ultrasonic anemometer. This will allow the validation of the equations developed in this work.

IX. FUTHER WORK

A refrigerated wind tunnel should be used to evaluate both the ice-free III NRG cup anemometer and the heated ultrasonic Gill anemometer under different icing conditions. In addition, work should be done to determine the minimum liquid water content at which the ice-free I and III NRG cup anemometers begin to collect ice.

X. ACKNOWLEDGMENT

This work was supported financially by the NSERC through a postdoctoral fellowship for the first author. We acknowledge the financial contribution of MDERR (Ministère du Développement Économique Régional et de la Recherché du Québec), TechnoCentre éolien Gaspésie -les-îles and Anti-icing Materials International Laboratory of Université du Québec à Chicoutimi and Wind Energy Group of Université du Québec à Rimouski. The authors particularly want to thank Jean Desrosiers of the TechnoCentre éolien Gaspésie-les-îles for his contribution to the completion of this work.

XI. REFERENCES

[1] Laakso, T., Holttinen, H., Ronsten, G., Tallhaug, L., Horbaty, R., Baring-Gould, I., Lacroix, A., Peltola, E., Tammelin, B., ″State-of-the-art of wind energy in cold climates" Wind Energy Production in Cold Climate, April 2003. Available: http://www.vtt.fi/virtual/arcticwind/publications.htm

[2] Tammelin, B., Cavaliere, M., Kimura, S., Morgan, C. and Peltomaa, A., ″Ice-free Anemometers, Proceeding of the International Conference", Wind Energy Production in Cold Climate, BOREAS IV, Published by: Finnish Meteorological Institute, Hetta, Finland, 31 March - 2 April 1998.

[3] Bengt Tammelin, Alain Heimo, Michel Leroy, Aulis Peltomaa and Jacques Rast, ″Ice-Free Wind Sensors – Results From the Eumetnet SWS II Project, Proceeding of the International Conference", Wind Energy Production in Cold Climate, BOREAS IV, Published by: Finnish Meteorological Institute, Hetta, Finland, 31 March - 2 April 1998.

[4] Aarnio, E., Partonen, S., ″Oprational Experience of Arctic Wind Farms", Proceeding of the International Conference, Wind Power Production in Cold Climate, BOREAS V, Published by: Finnish Meteorological Institute, Levi, Finland, 29 Nowember - 1 December 2000. Available: http://www.vtt.fi/virtual/arcticwind/publications.htm

[5] Botta, G., Cavaliere, M., Holttinen, H., ″Ice accretion at Acqua Spruzza and its effects on wind turbine operation and lose of energy production", Proceeding of the International Conference, Wind Energy Production in Cold Climate, BOREAS IV, Published by: Finnish Meteorological Institute, Hetta, Finland, 31 March - 2 April 1998. Available: http://www.vtt.fi/virtual/arcticwind/publications.htm

[6] Maissan, J. F., ″Wind Power Development in Sub-Artic Condition with Severe Rime Icing", Circumpolar Climate Change Summit and Exposition, Whitehorse, Yukon, Canada, March 19-21, 2001.

[7] Schönborg, A., Blomgren, L., ″Two year's experience of three different turbines on the same site - Rodovålen- in the very middle of Sweden", Proceeding of the International Conference, Wind Power Production in Cold Climate, BOREAS V, Published by: Finnish Meteorological Institute, Levi, Finland, 29 Nowember - 1 December 2000. Available: http://www.vtt.fi/virtual/arcticwind/publications.htm

[8] Schaffner B., ″Wind energy site assessment in harsh climatic conditions, Long term experience in Swiss Alps", Report METEOTEST, 2002. Available: http://www.vtt.fi/virtual/arcticwind/publications.htm

[9] Environment Canada web site, Available: http://www.climat.meteo.ec.gc.ca/Welcome_f.htm

[10] Walton, W. H. and Woolcock, A., ″The Suppression of Airborne Dust by Water Spray", International Journal Air Pollution, Vol. 3, pp. 129-153, 1960.

[11] Stallbrass, J.R., ″An appraisal of the single rotating cylinder method of liquid water content measurement", National research council of Canada, Nov. 1978.

[12] Anderson, D. N., ″Effect of Velocity in Icing Scaling", Tests, American Institute of Aeronautics and Astronautics, 29th Aerospace Sciences Meeting & Exhibit, Reno, Nevada, Paper AIAA-2000-0236, January 2000.

[13] Andesron, D. N. and Tsao, J.-C., ″Overview of Icing Physics Relevant to Scaling", American Institute of Aeronautics and Astronautics, 31th Aerospace Sciences Meeting & Exhibit, Reno, Nevada, Paper AIAA-2003-01-2130, January 2003.

[14] Jones K.F., ″The Density of Natural Ice Accretions", Fourth International Conference on Atmospheric Icing of Structure, E. D. F., volume 77, #1, pp. 114-118, Paris, September 1988.